INTERPRETATION AND RELIABILITY OF LABORATORY TESTS MEASURING POROSITY, PORE COMPRESSIBILITY, AND VELOCITY ON UNCONSOLIDATED DEEP OFFSHORE RESERVOIRS

Luc Pauget, F. Specia, and A. Boubazine, TOTALFINAELF

SUMMARY

The reliability of laboratory porosity and pore compressibility data obtained on unconsolidated (non-cemented) sands is a critical issue in heavy oil and deep-offshore reservoirs as initial pore volume and rock behavior during depletion can have a tremendous impact on production strategy and reserves.
The present experimental work first addresses the issue of sample integrity following the coring process: core damage is investigated by dedicated laboratory tests. Then, experimental work tackles elasto-visco-plastic behavior of unconsolidated reservoir sands and suggests an interpretation for creep phases and isotropic tests.

INTRODUCTION

The quantity of reserves in sand reservoirs, which represent most deep water and heavy oil targets, has imparted to petrophysical measurements on sands an importance it did not formerly have. Measurements on such facies involve techniques at the boundaries of two disciplines: soil mechanics for geotechnical engineering and rock mechanics for the oil industry. Geotechnical engineering developed models, tools and procedures to characterize non-cemented facies but performed no studies on representative low-ranges of stress. On the other hand, the oil industry is equipped to investigate far greater ranges of stress than those encountered in sand reservoirs, but measurements on non-cemented facies are considered skeptical. Indeed, the adequacy of such measurements has never been proven, and it is admitted that conventional under-stress measurement analyses are not valid since they are based on linear elasticity.

RESULTS – EXPERIMENTAL WORK

The following work is based on a large set of laboratory experiments on sand reservoirs and describes procedures that take into account sand sample specificity. It also shows that there are grounds for confidence in results provided by laboratory tests.

Sample Measurement Adequacy

The validity of laboratory measurements on sands is an issue that cannot be ignored. The recovery of cores representative of the formation state is called into question. Considering the drilling tool in the sandy formation, two types of damage can be encountered. First, the tool rotation could stir the grains and the torsion tensor could twist the soft core continuously. Figure 1 invalidates this assumption. It represents a CT Scan image of a damaged sand core. The orientation of visible lamination does not change along the core. Locally, the grain-to-grain contacts are not affected by the tool rotation.

Potential core twist has a low rotation frequency that is not observable at meter scale and, even less so, at sample scale. Secondly, the core could be affected by stress relaxation; the coring process is indeed quite violent and disturbing for poorly or non-cemented samples.

Figure 1. CT-Scan Image of a full diameter (15 cm) sand core.

The coring stress path is characterized by a sharp variation and inversion of the deviatoric stress which crosses the critical friction slope (in Mohr-Coulomb or Cam-Clay P'/Q representation) (Figure 2 and Figure 3).

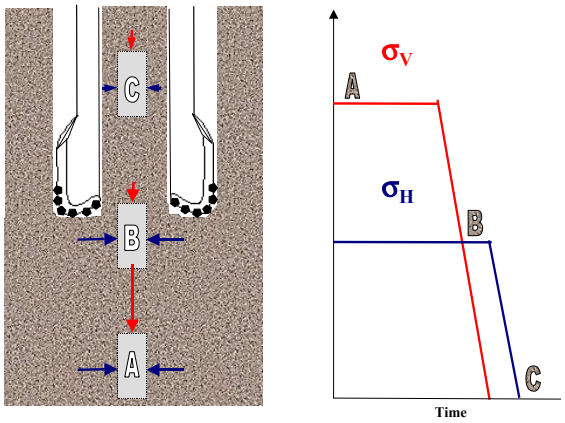

Figure 2. Drilling tool penetrating into formation and corresponding stress path.

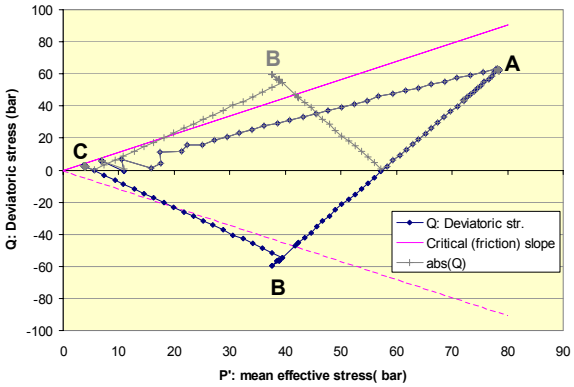

Figure 3. Representation of the stress path in P'/Q diagram.

To reproduce the equivalent coring stress path in the laboratory, a sand sample is taken as a reference. It is first set at reservoir conditions by applying the uniaxial strain stress path. Then, a stress path equivalent to the worst-case coring stress mentioned above is applied. Afterwards the sample is loaded again until it reaches reservoir stress and depletion is applied. The depletion performed under uniaxial strain conditions is representative of standard laboratory compaction tests. Further uniaxial unloading and isotropic loading cycles are also applied (Figure 4). Results, plotted in Figure 5, shows that sand behavior is obviously elasto-plastic and also agrees well with the Cam Clay description as during phase [A-B] (decrease of axial stress below radial stress and cross-over of critical slope) where the sample exhibits a swelling behavior (increase in volumetric strain). It also shows that hardening, which occurred during initial loading to reservoir conditions, is cancelled out by the coring stress path (complete softening). The consecutive loading [C-

A'] is not elastic. The sample has lost its "stress memory", which is nevertheless preserved by uniaxial or isotropic unloading (as can be observed on [A'-D-E]).

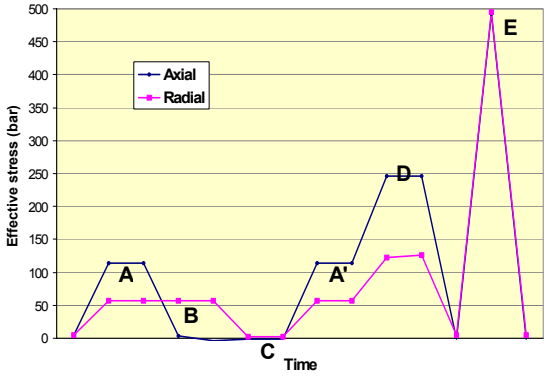

Figure 4. Stress path applied

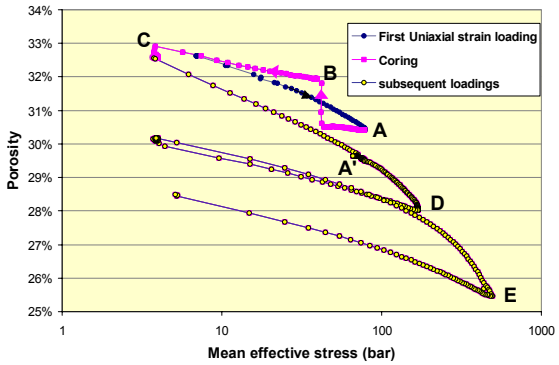

Figure 5. Volumetric strain observed during first loading to in-situ stress, coring process and subsequent reloadings

Conversely, if the derivative curve is now considered, (Figure 6) the coring stress path does not affect the results obtained from compaction tests. The measured pore compressibility during the first loading ("virgin" plastic compressibility) is fully consistent with that measured during phases [C-A'] and [A'-D].

The elastic compressibility is not well measured before the coring process; an order of magnitude is provided by the beginning of phase [A-B] and by the end of phase [B-C]. However, the elastic behavior can also be investigated using compressional wave velocity. The axial velocity is measured throughout the entire test. The results are plotted on Figure 7 versus an appropriate stress parameter (effective stress in the propagation axis). The different curves before and after coring, during loading and unloading phases and uniaxial and isotropic phases are superimposed. The elastic property does not change during the test. The disturbance of grain structure leads afterwards to a higher capacity of the grains to rearrange themselves during the first stage of second loading to reservoir conditions. Consequently, initial porosity after coring is lower than the previous porosity, but the samples recover their mechanical properties.

Influence of Loading Rate

One of the most outstanding characteristics of non-cemented samples is their viscous behavior. The amount of strain observed during creep phases renders the measured compressibility dependent on the test-loading rate. In the oil industry, the problem is either ignored or tackled by using very long testing times with loading rates approaching the true depletion rate (about 10 bars per year). (Ostermeier (7)). This section investigates a third way, which consists of performing a test that is not as time-consuming and corrects for the loading rate.

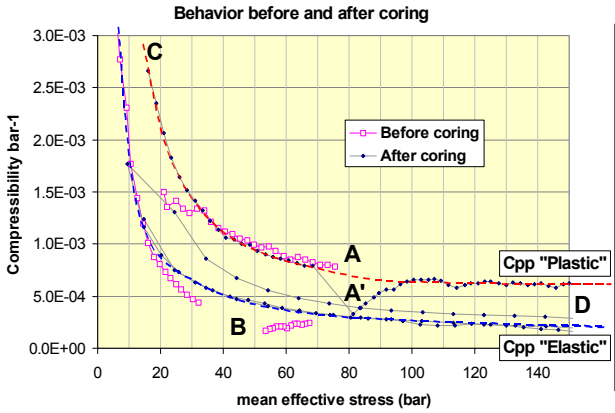

Figure 6. Velocity variation during testing.

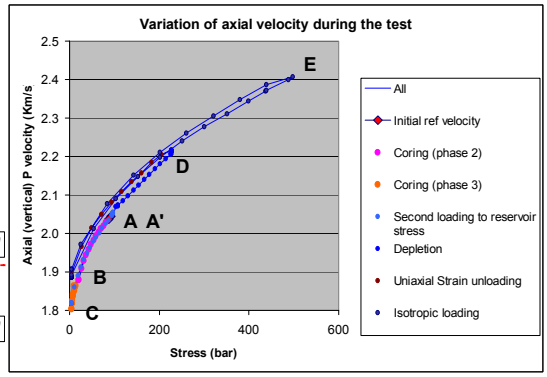

Figure 7. Compressibility variation during testing.

The creep and loading rate effect has been well investigated in literature. Two types of models are used to describe the creep strain curve. $\varepsilon = f(\frac{t}{\tau})$ where ε is the volummic strain; t is the time of creep and τ a characteristic rating time. The first is a logarithmic law: $\varepsilon = A.\ln(1+\frac{t}{\tau})$ (Sheidegger (1970) (6), De Waal (1994) (2), Hamilton & Shafer (3), Andersen (1)). The second is a normalized model with a finite maximum strain ε_f, a fractional power law: $\varepsilon = \dfrac{\varepsilon_f}{1+\left(\dfrac{t}{\tau}\right)^{\alpha}}$. (Dudley 1994 (4)).

The laboratory performed hundreds of creep analyses on reservoir samples under isotropic and uniaxial strain conditions. The creep time varied from 1 to 30 days. The best fit for creep behavior is clearly obtained with the logarithmic law. The following graphs present a creep phase studied on a reservoir sand sample (32% PV; 1 Darcy @ reservoir stress). Strain is obtained by two independent measurements: expelled pore volume and length variations. The test is performed under isotropic stress at 128 bars of effective stress. Creep is first analyzed for 24 hours (Figure 8). The two models provide quite suitable fits. Secondly, the same creep is now observed after 30 days (Figure 9). The two previous fits are chosen. The logarithmic-law based model provides a good prediction of the creep behavior throughout the duration of the test whereas measured strain exceeds the maximum stress limit given by the second model (ε_f = 2.3% and measured pore volumetric strain is 2.5 after one month). The reader should note that even if the logarithmic law may appear to be unrealistic as it leads to infinite strain, the results it provides are not inconsistent, even at the age of the earth (Figure 10). If model two is used to fit the long-term behavior of the creep with a recommended rating time of 10 years (Figure 11), extrapolated porosity range nears that predicted by the first model.

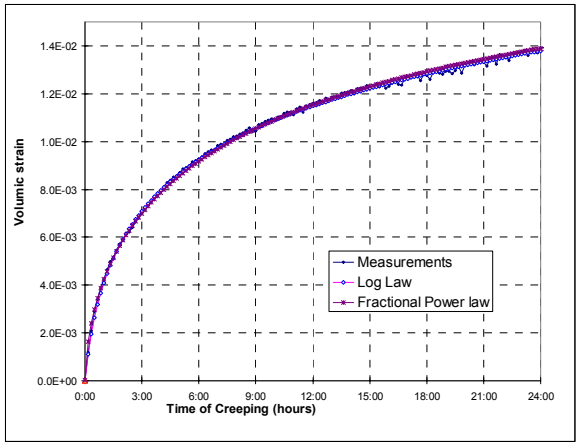

Figure 8. Creep Curve observed during 1 day.

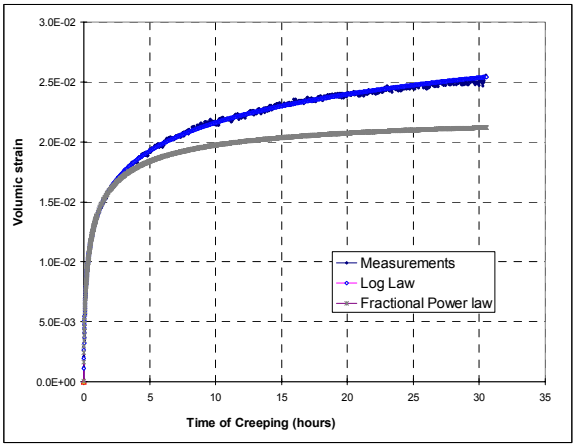

Figure 9. Same Creep observed during 30 days.

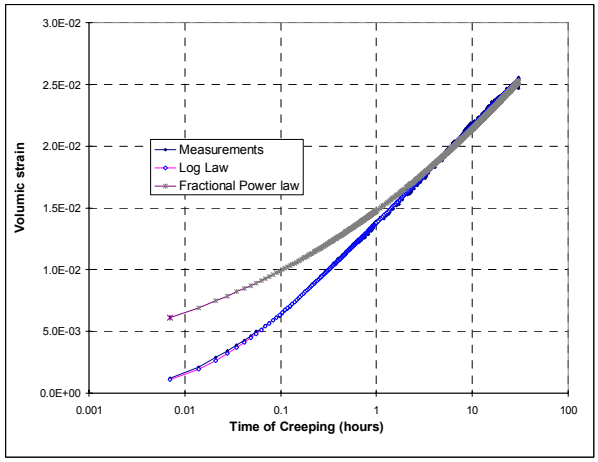

Figure 10. Creep Curve fitted by the second model, ignoring the first data (3 first days)

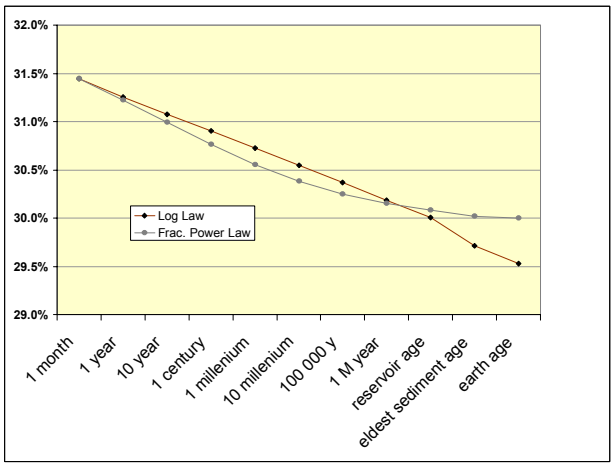

Figure 11. Extrapolation of creep behavior according to the model, at considerable times.

The logarithmic law was therefore selected for describing creep behavior. The creep curve is fitted using De Waal's law. The fit provides a dimensionless coefficient, b. The validity of this analysis is first validated with tests involving creep at different stresses (Figure 12). The illustrated example is a test performed on reservoir sand. Creep follows plastic loading at each stage. The measured value of b does not change with the stress (Figure13). The coefficient b can be considered as an intrinsic parameter of the rock that is valid within the range of stresses found in the non-cemented sand field [40b-300b].

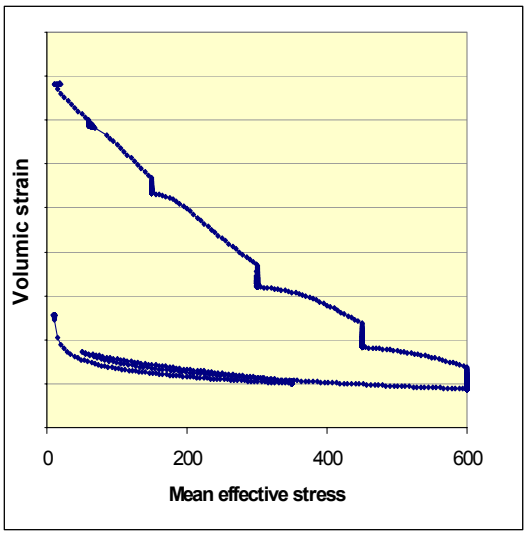

Figure 12. Compaction test on sand interrupted by creep phases.

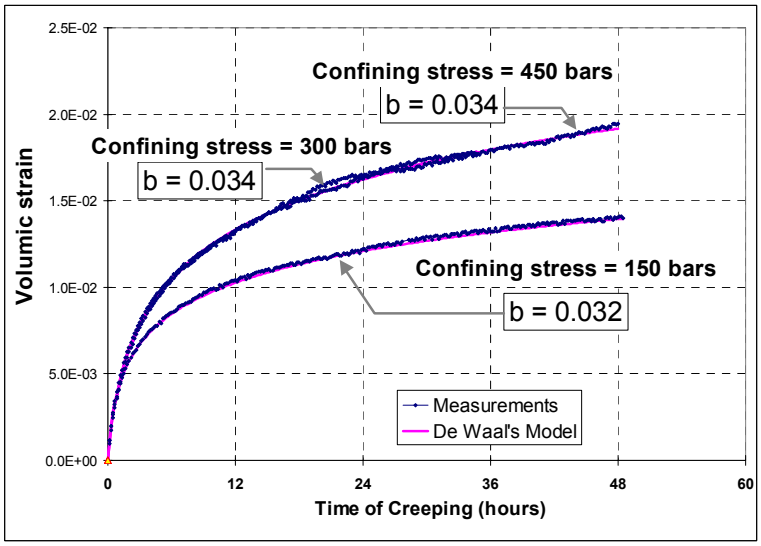

Figure 13. Interpretation of creep for different stress levels (curves @ 300 and 450 bars are superimposed).

Once these parameters are defined, De Waal's equations are used to correct the measured compressibility and to calculate compressibility for any loading rate. This calculation is put to the test by performing experiments with decreasing hydrostatic loading rates (Figure 14). The loading rate varies by a ratio of 1 to 100 (60/h, 6b/h, and 0.6b/h). Compressibility is measured throughout the test, and then the corrected compressibility is calculated to transform the "fast" compaction curves to "slower" ones (Figure 15). The calculation provides very good agreement between the corrected compressibility and the measured one, despite the relatively low correction that is applied (6% for a ratio of 10;

12% for a ratio of 100). In this case, the creep coefficient b used for the correction is the average coefficient found for the field: b = 0.024.

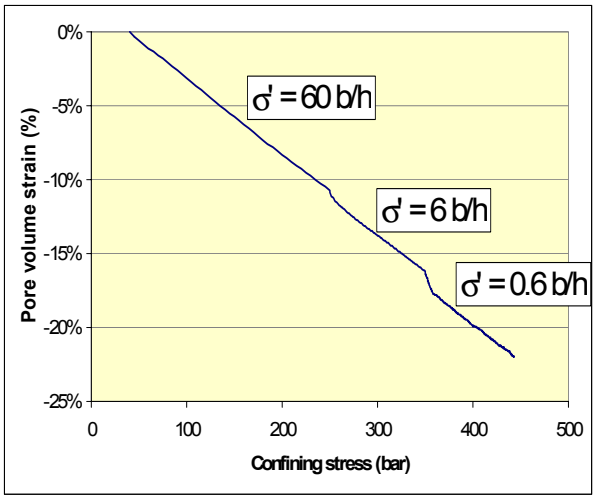

Figure 14. Compaction test with decreasing loading rate.

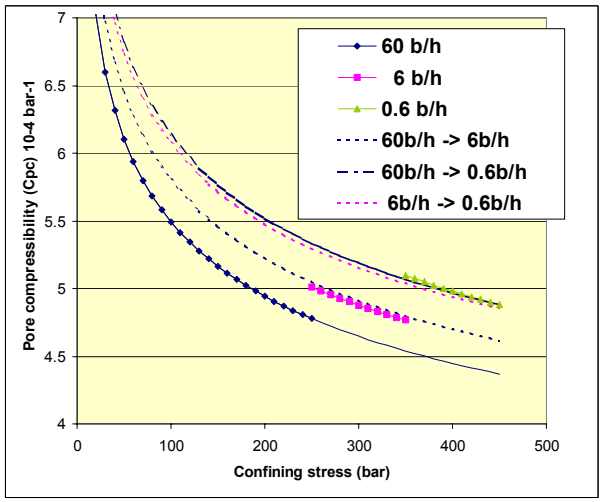

Figure 15. Measured compressibility (dots) and compressibility extrapolated and corrected for loading rate.

The slowest loading rate, 0.6b/h or 15 b/day, is close to the actual well testing loading rate. It is observed that another step ratio of 1 to 100 (0.15 b/day to 50 b/year) is on the order of magnitude of actual depletion rates. It should be added that the log behavior was not invalidated as far as it has been tested and that the strain observed over a period of 1 month represents about 75% of the total strain for creep lasting one year, according to the logarithmic law.

This set of tests provides confidence in the loading rate correction applied. It suggests that a good practice is to systematically perform a compaction test with regular loading followed by a stabilization phase where the creep is calibrated. It also clearly appears that, in any case, it is worse to not correct the results from standard compaction test sands than to assume that the loading rate correction can be extrapolated to actual reservoir depletion rate.

Correction of Isotropic Test

The stress path followed to measure compaction is another tricky issue in the case of sand samples. If a complete geomechanical model of the reservoir and its surrounding formation is not available, and it rarely is, the stress path at a point in the reservoir during depletion is not well known. It is admitted, and field simulations also confirm this, that the stress path inside the strained reservoir is close to a uniaxial path (vertical strain without radial deformations). Such oedometric tests are performed in the laboratory, even though most of the available results are derived from hydrostatic tests. Hydrostatic tests are also easier to perform and less expensive. And in addition, most local laboratories are not equipped for such tri-axial experiments.

In the case of cemented samples, the theory of poro-elasticity provides a very good approximation of pore compressibility under uniaxial strain conditions, obtained from measured Cpc pore compressibility under isotropic confining conditions:

$$C_{pp}^{oedo} = C_{pc}\left(1-\frac{2\alpha(1-2\nu)}{3(1-\nu)}\right) - C_S \quad [1]$$

Assuming that for the sand a= 1 and that grains are incompressible.

$$C_{pp}^{oedo} = C_{pc}\left(1-\frac{2(1-2\nu)}{3(1-\nu)}\right) = C_{pc}\left(\frac{(1+\nu)}{3(1-\nu)}\right) \quad [2]$$

The sand behavior is clearly not elastic but elasto-visco-plastic. It may be of interest to examine models derived from thermo-plasticity developed for soil mechanics. One of the most widely-used models is the Cambridge or Cam Clay Model. In its basic version, the Yield locus (the surface that defines the elastic and plastic domains) and the plastic potential (function that governs the plastic strain evolution) are related.The Yield Locus is given by:

$$f(Q,P',M) = M^2P'^2 + 2MPcrP' + Q^2 = 0 \quad [3]$$

where P' is the mean effective stress, Q the deviatoric stress and Pcr the hardening parameter (Pcr = P'max/2 in the isotropic Q=0 line), M the critical slope
The stress-strain relations are defined by:

$$p' = p'_0\, e^{Ko\left(\varepsilon_{kk}^e - \varepsilon_{kk0}^e\right)} \text{ and } P_{cr} = P_{cr_0} e^{k\left(\varepsilon_{kk}^p - \varepsilon_{kk0}^p\right)} \quad [4]$$

where ε_{kk}^e, $\varepsilon_{kk_0}^e$, ε_{kk}^P, $\varepsilon_{kk_0}^P$ are the current and initial; elastic and plastic volumetric strain, respectively.

K and k_0 are constants that can be written as: $k_0 = \frac{1+e_0}{\kappa}$ and $k = \frac{1+e_0}{\lambda-\kappa}$, where e_0 is the initial void ratio, which is linked to initial porosity ϕ_0 by: $e_0 = \frac{\phi_0}{1-\phi_0}$. κ and λ are material constants termed swelling and compressibility coefficients, respectively.

According to the model, the ratio Q/P' is constant in an oedometric stress path. This assumption is validated for sand reservoirs by a large number of experiments. In Figure 17 the stress path measured during a compaction test which includes the isotropic, deviatoric and oedometric stress paths is shown in the plane P'-Q. It must be pointed out that during oedometric phases (phase 3, 4, 5), the radial pressure is not a set point. It is derived from the uniaxial strain boundary condition. Figure 16 illustrates that even when the oedometric loading in the plastic area is interrupted by an unloading phase, Q varies such that the stress path returns to the previous Q/P slope when it again reaches the plastic domain. Hence, with equation [3], during oedometric loading in the plastic

domain, $\frac{Pcr}{Pcr_0} = \frac{P'}{P'_0}$. This is valid for any stress path in which Q/P' is constant and all the more so for an isotropic stress path. From [4] it is observed that ε_{kk}^{e} and ε_{kk}^{P} depend only on P'. Compressibility can therefore be calculated as:

$$C_{pp} = \frac{\partial Vp}{Vp_0 \partial p} = \frac{\partial Vb}{Vb_0 \phi_0 \partial p} = \frac{\partial}{\partial p}\left[\frac{Vb}{Vb_0 \phi_0}\right] = \frac{\partial \varepsilon_{kk}}{\partial p} = \frac{\partial}{\partial p}\left[\varepsilon_{kk}^{e} + \varepsilon_{kk}^{p}\right] = \frac{\partial}{\partial P'}\left[\varepsilon_{kk}^{e} + \varepsilon_{kk}^{p}\right]\frac{\partial P'}{\partial p} \qquad [5]$$

Assuming that for sand Biot's coefficient = 1, the isotropic stress path is $\frac{\partial P'}{\partial p} = -1$ and the oedometric stress path is $\frac{\partial P'}{\partial p} = -\frac{(1+2K'_0)}{3}$

where K'o is the ratio of the radial and axial effective stresses during oedometric loading.

From [5]: $C_{pp}^{Isotropic}(P') = C_{pp}^{oedometric}(P').\frac{(1+2K'_0)}{3}.$ [6]

In elasticity, the oedometric load is $\nu = \frac{K'_0}{(1+K'_0)}$ replacing it in [2] gives the same ratio between the compressibilities: $C_{pp}^{Isotropic}(P') = C_{pp}^{oedometric}(P').\frac{(1+2K'_0)}{3}$

The measured K'o coefficient varies between 0.4 and 0.6, but since 90% of the samples range from 0.45 to 0.55, the corresponding correction factor for isotropic compressibility varies from 0.63 to 0.7.

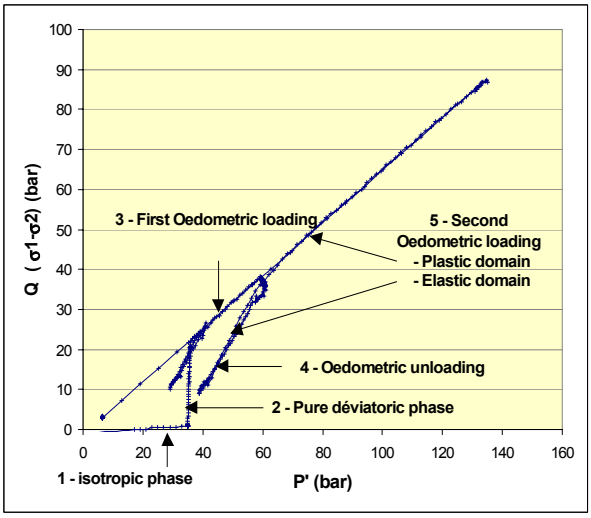

Figure 16. Compaction test including isotropic and oedometric stress paths.

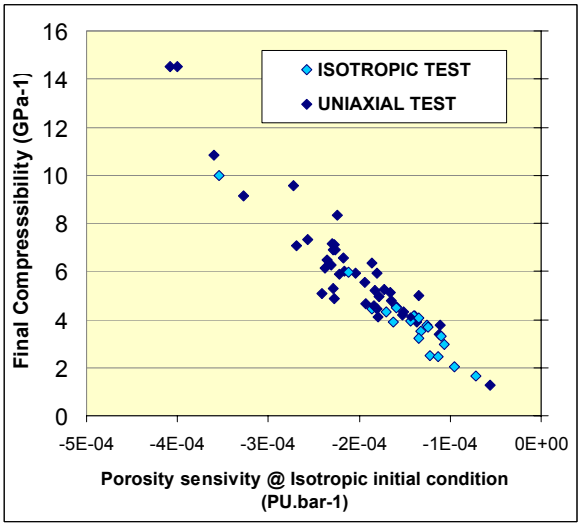

Figure 17. Comparison of oedometric and isotropic test using a common parameter.

It must be noted that the hardening law term was not used. The result obtained in [6] is valid for any hardening law in which strain can be expressed with P'.

At this stage it can be verified practically that the correction applied provides consistent results. Procedures for isotropic and oedometric tests have one common phase: an isotropic load up to initial mean effective reservoir stress (Phase 1 in Figure 16). The set of results obtained from the oedometric test shows that a correlation can be observed between the sensitivity of porosity to stress at initial conditions and the pore compressibility measured at the end of depletion. Using this relation isotropic tests are compared to the oedometric tests with a medium correction factor of 0.67 for the final measured compressibility (Figure 17). Results fit the trend. One may note that the samples tested under isotropic confining conditions have the lowest compressibility. Indeed, samples selected for isotropic tests are relatively well-sorted, fine sands.

In the Cam Clay model, the strain/stress relation in constant P'/Q loading is given by relations:

$\varepsilon_V = C.\ln\left(\frac{P'}{P_0}\right)$ where C = $\frac{\lambda}{(1+e_0)}$ is in the plastic domain and C = $\frac{\kappa}{(1+e_0)}$ in the elastic domain. Plotting C vs. ln(P'), it can be seen in the following example (Figures 18 and 19) that if κ is a material constant as expected, λ increases with pressure P' to a certain limit. Figure 18 represents a triaxial test that includes isotropic and oedometric phases, as described in Figure 16. The different loading phases are interrupted by stabilization phases. Consequently, transient behavior is observed during most of the subsequent loading. Nevertheless it appears that the different types of loading are consistent with a global plastic behavior which varies with P' only. Figure 19 shows two tests of the same type. They are compared against an isotropic test performed on a sample from the same layer. Once again, the different tests match the same overall behavior. This provides confidence in the assumption that the stress-strain relation can be expressed with P' only, and consequently, in the relation obtained between compressibility measured along isotropic and oedometric paths.

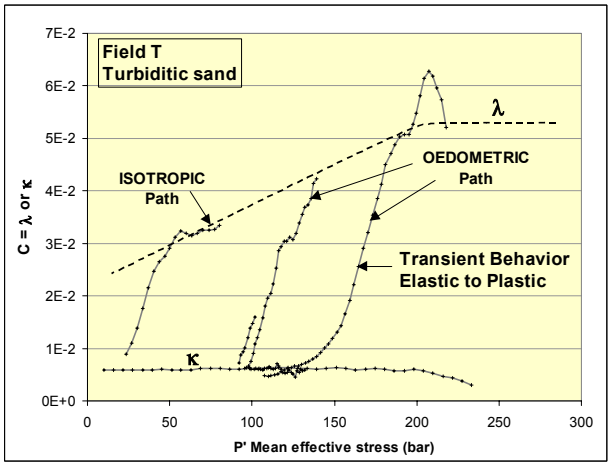

Figure 18. Variations in C during different types of loading for medium to coarse sands.

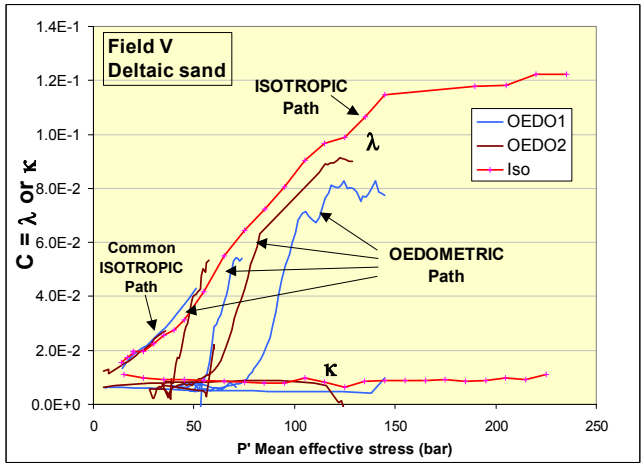

Figure 19. Comparison of the variation in C for three coarse sands from the same layer

DISCUSSION

The series of tests presented here confirm the specific elasto-visco-plastic behavior of reservoir sands. It also illustrates that though the various mechanical properties of sand are not fundamentally modified during the coring process, the measurement of these properties requires particular care in the test procedures and interpretation.

- First, the obvious hysteresis must be taken into account in reservoir simulations. The interpretation of a build-up well test, for instance, must be performed with a compressibility coefficient 4 to 10 times lower than the maximum plastic compressibility at the end of depletion. Hence, the interpretation of both virgin loading and unloading (or second loading) are necessary throughout the compaction test.
- Secondly, the mechanical properties vary with pressure. Therefore, it is helpful to apply continuous regular loading with small and frequent pressure steps associated with accurate strain measurements. Many steps reduce the amount of time spent waiting for strain stabilization (which can be long) at each step. The measured properties should be corrected for the time-dependent viscous effect.
- This viscous effect can be calibrated by analyzing the creep curves. The previous loading can then be reliably corrected.
- One drawback of stabilization is that it affects subsequent loading. Actually, observations during loading consist essentially of measuring the transient behavior between a pure elastic and a pure plastic mechanism. Considerable loading (larger than the maximum actual depletion) is therefore necessary to catch the pure plastic behavior. Conversely, it can be added that the actual reservoir may also behave this way either because the reservoir is over-consolidated (uplift, erosion) and/or because at production time scale, the previous geological load corresponds to a stabilization phase.
- Although more representative triaxial tests are preferable, isotropic testing can provide a suitable approximation of the compressibility under uniaxial strain conditions if the standard correction is used with a coefficient of 2/3 (K'o=0.5).

CONCLUSIONS

The conclusions of this work suggest that the mechanical properties of reservoir sand samples are not destroyed during the coring process and they can be measured in laboratory. However, observations made on these samples also reveal that the behavior of the reservoir sand strongly depends on the reservoir stress state. The consolidation state of the reservoir (the maximum stress during its geological history) cannot be measured from laboratory testing on sands. Yet, this is a critical parameter for the calibration of transient reservoir behavior during depletion. The following outstanding points may provide improvements.

– Development of a dilatometer that can perform in-situ measurements of the consolidation pressure.

- Measurements on reservoir shale such as those performed for soil mechanics studies. The shale, contrary to the sand, is presumed to conserve the "stress memory" of its previous loads. Some preliminary results are encouraging but need to be validated.
- Understanding creep micro mechanisms. The description of creep is based on experimental observation or analogies with simple systems (e.g. Kelvin model). This does not allow extrapolation to significantly large times. Only understanding of the sliding-crushing mechanism and the redistribution of the stress mechanism at the grain scale and its mathematical transcription could validate or invalidate the extrapolation of the log law observation to the geological age. This extrapolation also has great impact on the extent (the amount of pressure drop) of the actual transient behavior of the reservoir (between elastic to plastic), and consequently, on the energy (natural pressure support by the Work of the force of gravity of overburden) that could be expected from compaction.

REFERENCES

1. Andersen M. A., N. Fogad, and H. F. Pedersen, "The rate compaction-type compaction of a weak North Sea Chalk," Rock Mechanics Proceedings of the 33rd U.S Symposium, Balkkema (1992)
2. DE WAAL, J. A., "On the rate type compaction behaviour of sandstone reservoir rock," Thesis Delft University of Technology, Netherlands 1986.
3. Hamilton J. M. and Shafer J. L., "Measurement of pore compressibility characteristics in rock exhibiting pore collapse and volumetric creep," SCA Conference Paper Number 9124 (1991).
4. Dudley II, J. W., M. T. Myers, R. D Shew, and M. M. Arasteh, "Measuring compaction and compressibilities in inconsolidated reservoir materials via time-scaling creep," Eurock'94, Rotterdam '1994 & SPE Reservoir Evaluation & Engineering. October 1998.
5. Magnan, J. P. "Le rôle du fluage dans les calculs de consolidation et de tassement des sols compressibles," Bull. liaison Labo. P. et C., 180, juil-août (1992).
6. Scheidegger, A. E., "On the rheologie of rock creep." Rock Mechanics, 2, 138-145 (1970).
7. Ostermeier, R. M., "Compaction Effects on Porosity and Permeability: Deepwater Gulf of Mexico Turbidites," February 2001 Society Of Petroleum Engineers SPE Distinguished Author series, SPE 26468 –1993.
8. Charlez, Ph. A., "Rock Mechanics - Petroleum Applications," Editions Technip (1997).
9. Biot, M. A., and D. G. Willis, "The elastic coefficients of the theory of consolidation," J. Applied Phy., 1957.
10. Zimmerman, R. W., W. H. Somerton, and M. S. King, "Compressibility of porous rocks," J. Geophysical research, vol 91, n°B12, pp 12765-12777, 1986.